

Reconfigurable Intelligent Surface (RIS): Beamforming, Modulation, and Channel Shaping

Viva Presentation

Yang Zhao, supervised by Prof Bruno Clerckx

Department of Electrical and Electronic Engineering
Imperial College London

May 2, 2024

Do we want more waves in the air?

Massive MIMO is here



(a) 8T8R and mMIMO at Imperial



(b) Cellular statistics

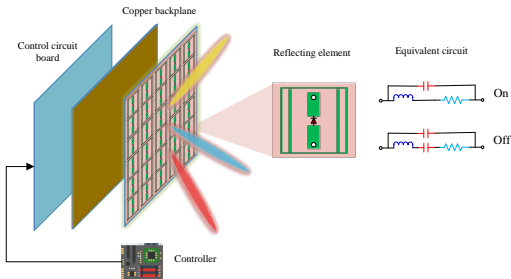
How far are we from the Shannon capacity?

$$C(\mathbf{H}) = \max_{\mathbf{Q} \succeq 0, \text{tr}(\mathbf{Q}) \leq P} \log \det \left(\mathbf{I} + \rho \mathbf{H} \mathbf{Q} \mathbf{H}^H \right)$$

- Modulation, coding, and beamforming to adapt to the stochastic channel
- Reconfigurable Intelligent Surface (RIS) can **shape and control** the channel

What is RIS?

A planar surface of controllable scattering elements for signal amplitude and phase manipulation [1].

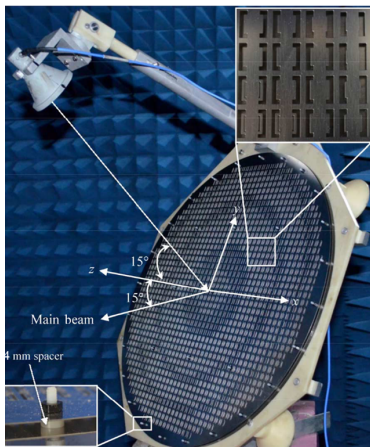


Characteristics

- Low-power and low-cost
- Negligible noise and latency
- Full-duplex without self-interference
- Programmable in real-time

Ancestor of RIS: Reflectarray antenna

A reflectarray antenna consists of an array illuminated by a feeding antenna [2].

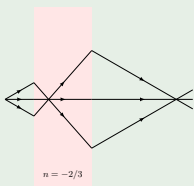


A progressive phase shift can be applied to the unit cells (a.k.a. elements) to steer the beam direction.

What is the difference in RIS?

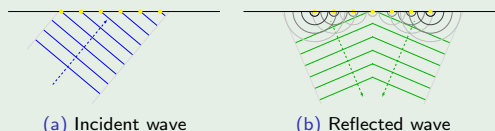
- ① Metamaterial enables **real-time control** and **unconventional behavior**.
- ② Impinging waves can be **partially refracted** and **reflected**.
- ③ The feed can be **mobile** while the surface is **scalable** and **multi-functional**.
- ④ Elements can be physically interconnected for **cooperative wave scattering**.

Refraction



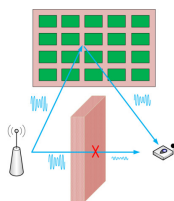
- Negative index material can focus waves
- Amplitude and phase responses can be tuned by diodes and FPGA
- Similar for wave reflection

Reflection

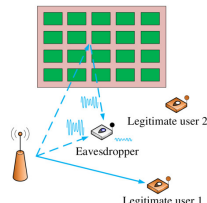


Use case: Beamforming

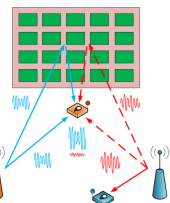
Beamforming of RIS and transceiver can be jointly designed for a specific performance measure [1].



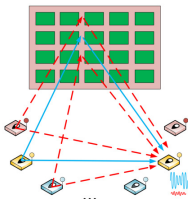
(a) Coverage extension



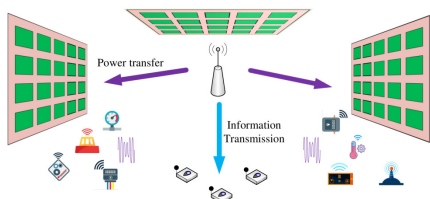
(b) Security enhancement



(c) Interference mitigation



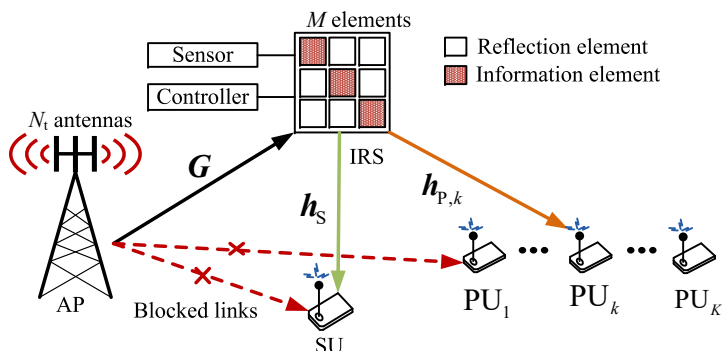
(d) Assist D2D network



(e) Assist information and power transfer

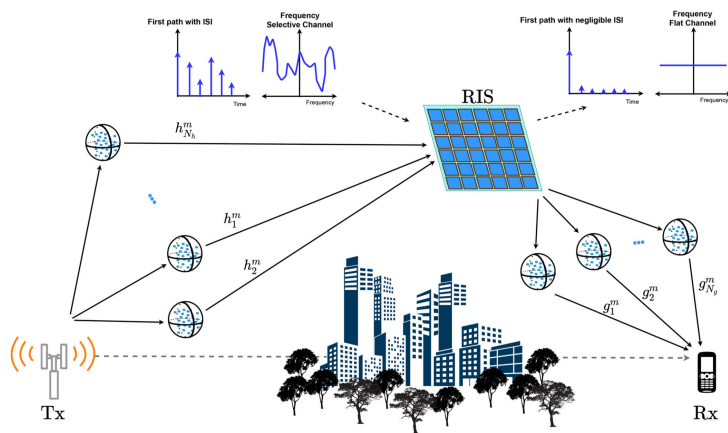
Use case: Modulation

RIS can be used for backscatter **modulation** by periodically switching the reflection pattern [3].



Use case: Channel shaping

Channel shaping exploits the RIS as a stand-alone device to modify the inherent properties of the propagation environment [4].



RIS-aided SWIPT: Joint waveform and beamforming design

Overview

- *What does this paper propose?*

A single-user multi-carrier Simultaneous Wireless Information and Power Transfer (SWIPT) system aided by a passive RIS.

- *How does it differ from previous work?*

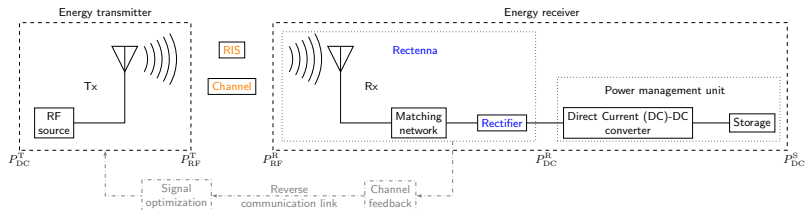
We consider waveform and beamforming design for practical receiver architectures under non-linear harvester and frequency-flat RIS models.

- *What are the benefits?*

It exploits the spatial-frequency domain and rectifier behavior to enlarge the Rate-Energy (R-E) region, achieving squared asymptotic performance than conventional designs.

WPT via radio waves

Categories	Medium	Device	Power level	Frequency	Range
Near-field	Magnetic resonant coupling	Resonators	Up to 10 W	kHz – MHz	m
	Inductive coupling	Wire coils	Up to 10 W	Hz – MHz	cm
	Capacitive coupling	Metal plates	Up to 1 W	kHz – MHz	mm
Far-field	Radio-Frequency (RF) wave	Rectenna	$\mu\text{W} - \text{mW}$	MHz – GHz	m
	Light wave	Laser	$\mu\text{W} - \text{mW}$	THz	km



The end-to-end Wireless Power Transfer (WPT) efficiency is

$$\eta = \frac{P_{\text{DC}}^{\text{S}}}{P_{\text{DC}}^{\text{T}}} = \underbrace{\frac{P_{\text{RF}}^{\text{T}}}{P_{\text{DC}}^{\text{T}}}}_{\eta_1} \underbrace{\frac{P_{\text{RF}}^{\text{R}}}{P_{\text{RF}}^{\text{T}}}}_{\eta_2} \underbrace{\frac{P_{\text{DC}}^{\text{R}}}{P_{\text{RF}}^{\text{R}}}}_{\eta_3} \underbrace{\frac{P_{\text{DC}}^{\text{S}}}{P_{\text{DC}}^{\text{R}}}}_{\eta_4}$$

where η_2 and η_3 models the channel and rectenna, respectively.

Received signal and harvested power

The rectenna efficiency η_3 depends on its input waveform (power and shape).

Rectenna model

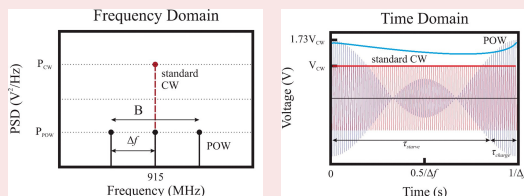
- Linear region (constant η_3): $P_{DC}^R = \eta_3 P_{RF}^R = \eta_3 \mathbb{A}\{|y(t)|^2\}$
- Non-linear region: Taylor expansion on diode characteristic equation

$$\arg_{x(t)} \max P_{DC}^R = \arg_{x(t)} \max z \triangleq \sum_{i=2, \text{even}}^{n_0} \beta_i \mathbb{A}\{y^i(t)\},$$

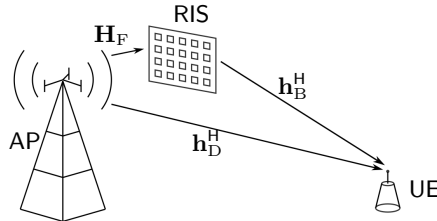
where $\beta_i = I_S \frac{R_A^{i/2}}{i!(nv_T)^i}$ is a constant and n_0 is the truncation order.

In multi-carrier WPT ...

- $n_0 \geq 4$ allows components to compensate each other for higher DC power
- High Peak-to-Average Power Ratio (PAPR) (e.g., multi-sine) is preferred [5]



From WPT to RIS-aided SWIPT



- SWIPT features shared signal, spectrum, and infrastructure
- RIS enhances the RF-to-RF efficiency η_2 which has been a major concern

Transmit waveform

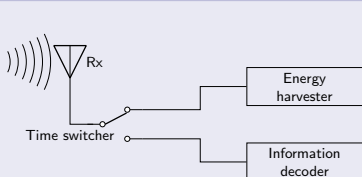
$$\mathbf{x}(t) = \Re \left\{ \sum_{n=1}^N \left(\mathbf{w}_{I,n} \cdot \underbrace{\tilde{x}_{I,n}(t) e^{j2\pi f_n t}}_{\text{modulated}} + \mathbf{w}_{P,n} \cdot \underbrace{e^{j2\pi f_n t}}_{\text{multi-sine}} \right) \right\}$$

Frequency-flat RIS model

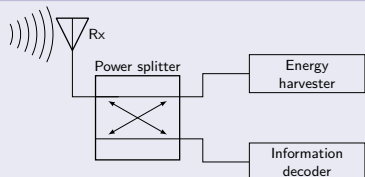
$$\mathbf{h}_n^H = \mathbf{h}_{D,n}^H + \mathbf{h}_{B,n}^H \boldsymbol{\Theta} \mathbf{H}_{F,n}$$

Performance analysis

Receiver architectures



(a) Time Switching (TS) receiver



(b) Power Splitting (PS) receiver

Rate-Energy (R-E) region of PS

$$R(\boldsymbol{\theta}, \mathbf{w}_I, \rho) = \sum_{n=1}^N \log_2 \left(1 + \frac{(1-\rho)|\mathbf{h}_n^\text{H} \mathbf{w}_{I,n}|^2}{\sigma_n^2} \right),$$

$$z(\boldsymbol{\theta}, \mathbf{w}_I, \mathbf{w}_P, \rho) = \sum_{i=2, \text{even}}^{n_0} \beta_i \rho^{i/2} \mathbb{E} \left\{ \mathbb{A} \left\{ y^i(t) \right\} \right\},$$

$$\mathcal{C}_{\text{R-E}}(P) \triangleq \left\{ (r, e) : 0 \leq r \leq R, 0 \leq e \leq z, \|\mathbf{W}_I\|_F^2/2 + \|\mathbf{W}_P\|_F^2/2 \leq P \right\}$$

Joint waveform and beamforming design

Problem formulation

$$\begin{aligned} & \max_{\boldsymbol{\theta}, \mathbf{W}_I, \mathbf{W}_P, \rho} \quad z(\boldsymbol{\theta}, \mathbf{W}_I, \mathbf{W}_P, \rho) \\ \text{s.t.} \quad & \|\mathbf{W}_I\|_F^2/2 + \|\mathbf{W}_P\|_F^2/2 \leq P, \\ & R(\boldsymbol{\theta}, \mathbf{W}_I, \rho) \geq \bar{R}, \\ & |\phi_l| = 1, \quad l = 1, \dots, L, \\ & 0 \leq \rho \leq 1, \end{aligned}$$

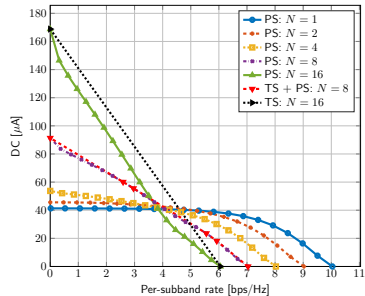
Solution by Block Coordinate Descent (BCD)

- Optimally decouple the spatial and frequency domain design

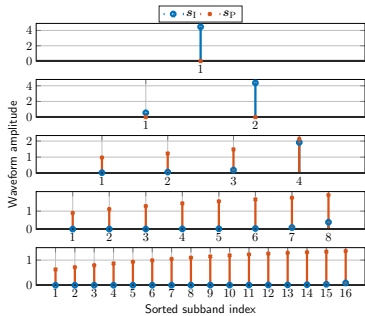
$$\mathbf{W}_{I/P,n} = \underbrace{s_{I/P,n}}_{\text{frequency}} \underbrace{\mathbf{p}_{I/P,n}}_{\text{spatial}}$$

- Active beamforming \mathbf{p} : Maximum Ratio Transmission (MRT)
- Passive beamforming $\boldsymbol{\theta}$: Successive Convex Approximation (SCA)
- Power allocation s and splitting ratio ρ : Geometric Programming (GP)

Simulation results: Number of subbands N



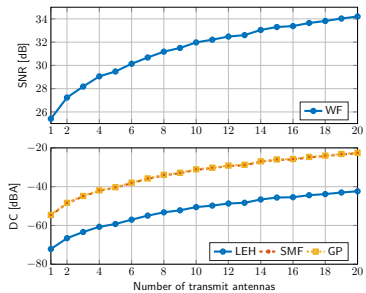
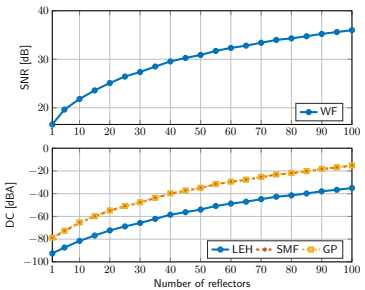
(a) R-E region



(b) Waveform amplitude

- Increasing N reduces per-subband rate but boosts harvested energy
- Region is convex at small N (favors PS) and concave at large N (favors TS)
- Dedicated multi-sine power waveform is unnecessary at small N

Simulation results: Asymptotic behavior

(a) Number of transmit antennas M (b) Number of RIS elements L

- Active beamforming: array gain M and harvested power order M^2
- Passive beamforming: array gain L^2 and harvested power order L^4
- Superlinear thanks to coherent scattering and rectifier nonlinearity

RISscatter: Unifying Backscatter Communication (BackCom) and RIS

Overview

- *What does this paper propose?*

RISscatter — a batteryless cognitive radio that recycles ambient signal in an adaptive and customizable manner.

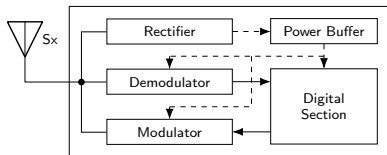
- *How does it differ from previous work?*

Backscatter modulation and passive beamforming are seamlessly integrated from the perspective of probability distribution.

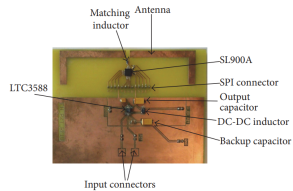
- *What are the benefits?*

It supports cooperative and distributed deployment, avoids complex architecture and signal processing, and can be built over legacy systems.

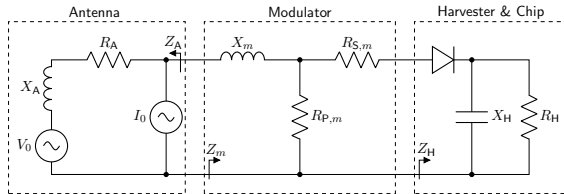
Node architecture



(a) Block Diagram



(b) RFID tag with harvester [6]



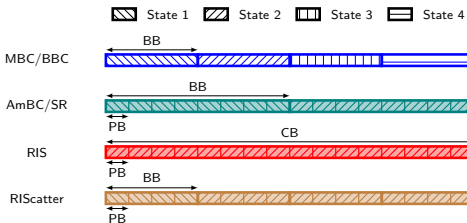
(c) Equivalent Circuit

Impinging waves can be used for powering, modulation, and beamforming.

Reflection coefficient

The node changes state by switching load impedance (and reflection coefficient)

$$\Gamma = \frac{Z_L - Z_0^*}{Z_L + Z_0}$$



- RIS: the state at a specific time is known (as a passive beamforming codeword) to the transceiver

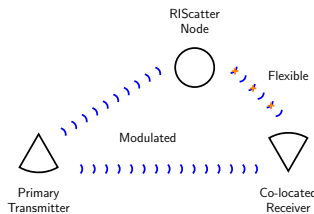
$$\Gamma_m = \exp(j\phi_m),$$

- BackCom: all states occur with equal probability (as part of information codeword) to be detected at the receiver

$$\Gamma_m = \alpha_m \frac{c_m}{\max_{m'} |c_{m'}|},$$

RISscatter system

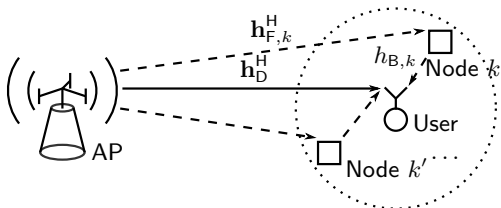
	Backscatter	Ambient backscatter	Symbiotic radio	RIS	RISscatter
Information link(s)	Backscatter	Coexisting	Coexisting	Primary	Coexisting
Primary on backscatter	Carrier	Multiplicative interference	Spreading code	—	Energy uncertainty
Backscatter on primary	—	Multiplicative interference	Channel uncertainty	Passive beamforming	Dynamic passive beamforming
Cooperative devices	—	No	Transmitter and receiver	—	Transmitter, nodes, and receiver
Sequential decoding	—	No	Primary-to-backscatter	—	Backscatter-to-primary
Reflection pattern by	Information source	Information source	Information source	Channel	Source, channel, and priority
Input distribution	Equiprobable	Equiprobable	Equiprobable or Gaussian	Degenerate	Flexible
Load-switching speed	Fast	Slow	Slow	Quasi-static	Arbitrary



- **Primary link:** active legacy transmission from an RF source
- **Backscatter link:** passive free-ride transmission from RISscatter nodes

RISscatter renders the node input distribution as a function of information source, Channel State Information (CSI), and priority of coexisting links.

Signal model



Within each backscatter block, received signal at primary block n is

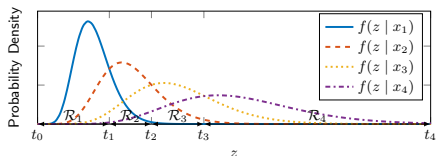
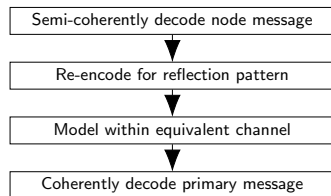
$$y[n] = \underbrace{\left(\mathbf{h}_D^H + \sum_k \alpha_k \mathbf{h}_{C,k}^H \textcolor{orange}{x_k} \right)}_{\mathbf{h}^H(\textcolor{orange}{x_C})} \mathbf{w} s[n] + v[n],$$

Properties

- ① Primary and backscatter symbols are superimposed by double modulation
- ② Backscatter signal is much weaker due to double fading
- ③ The spreading factor (i.e., symbol period ratio N) is usually large
- ④ Each state is simultaneously part of information and beamforming codeword
- ⑤ Reflection pattern over time is guided by input probability distribution

Low-complexity receiver

We propose a low-complexity receiver that exploits the aforementioned properties to avoid Successive Interference Cancellation (SIC).



- Accumulated receive energy $z = \sum_n |y[n]|^2$ follows Gamma distribution
- **Backscatter detection** under primary uncertainty is part of **channel training**
- Requires one energy comparison and re-encoding per backscatter symbol (much simpler than symbiotic radio with N SIC and 1 combining)

Joint beamforming, input distribution, and energy detector design

Achievable rate

$$\sum_k R_{B,k} = \sum_{m_K} P_K(x_{m_K}) \sum_{m'_K} P(\hat{x}_{m'_K} | x_{m_K}) \log P(\hat{x}_{m'_K} | x_{m_K}) / P(\hat{x}_{m'_K})$$
$$R_P = \sum_{m_K} P_K(x_{m_K}) N \log \left(1 + \frac{|\mathbf{h}^H(x_{m_K})\mathbf{w}|^2}{\sigma_w^2} \right)$$

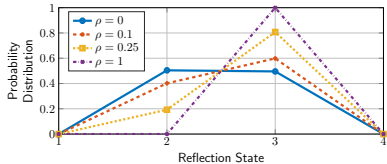
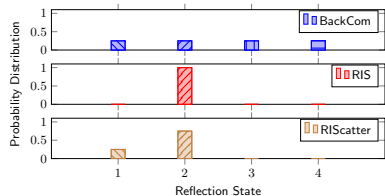
Problem formulation

$$\max_{\{\mathbf{p}_k\}, \mathbf{w}, \mathbf{t}} \quad \rho R_P + (1 - \rho) \sum_k R_{B,k}$$
$$\text{s.t.} \quad \mathbf{1}^T \mathbf{p}_k = 1, \quad \mathbf{p}_k \geq \mathbf{0}, \quad \forall k,$$
$$t_{l-1} \leq t_l, \quad t_l \geq 0, \quad \forall l,$$
$$\|\mathbf{w}\|^2 \leq P,$$

Solution by Block Coordinate Descent (BCD)

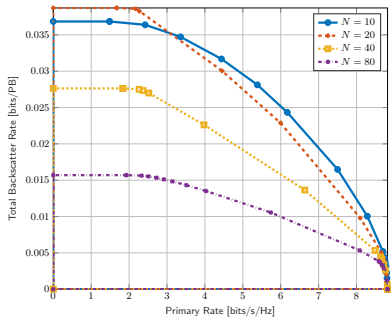
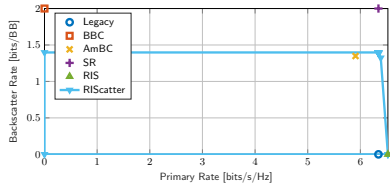
- Input distribution $\{\mathbf{p}_k\}$: Karush-Kuhn-Tucker (KKT)
- Active beamforming \mathbf{w} : Projected Gradient Ascent (PGA)
- Energy decision threshold \mathbf{t} : Dynamic Programming (DP)

Simulation results: Input distribution



- BackCom and RIS are special cases of RISscatter with uniform and degenerate input distribution
- Increasing ρ from 0 to 1 creates a smooth transition from backscatter modulation to passive beamforming

Simulation results: Rate region



- RISscatter backscatter rate is lower than symbiotic radio (due to energy detection) but higher than ambient backscatter (due to adaptive encoding)
- A large spreading factor N improves backscatter BER but reduces data rate
- Active and passive transmission can share resource with mutual benefits

Channel shaping using RIS: From diagonal model to beyond

Overview

- *What does this paper study?*

To what extent can a passive RIS redistribute the singular values of a Multiple-Input Multiple-Output (MIMO) channel.

- *How does it differ from previous work?*

We consider a Beyond-Diagonal (BD) architecture, depict the singular value region, derive analytical bounds, and solve the rate maximization problem.

- *What are the benefits?*

Channel shaping is ubiquitous for communication, sensing, and power transfer, which helps to decouple the RIS-transceiver design. We also propose an efficient and universal BD-RIS design framework.

Wave scattering model

Diagonal RIS

Each element acts as an individual scatterer with phase shift only

$$\boldsymbol{\Theta} = \text{diag}(\theta_1, \dots, \theta_{N_S}) = \text{diag}(e^{j\phi_1}, \dots, e^{j\phi_{N_S}})$$

BD-RIS

Each group contains L connected elements, allowing amplitude and phase control

$$\boldsymbol{\Theta} = \text{diag}(\boldsymbol{\Theta}_1, \dots, \boldsymbol{\Theta}_G), \quad \boldsymbol{\Theta}_g^H \boldsymbol{\Theta}_g = \mathbf{I}_L, \quad \forall g$$

- *Subchannel rearrangement*: allows each group to rearrange and combine the backward and forward subchannels by strength

$$\sum_{n=1}^{N_S} |h_{B,n}| |h_{F,n}| \rightarrow \sum_{g=1}^G \sum_{l=1}^L |h_{B,\pi_{B,g}(l)}| |h_{F,\pi_{F,g}(l)}|$$

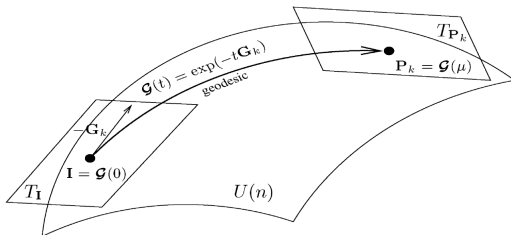
- *Subspace alignment*: rotate backward-forward (intra-group, multiplicative) and direct-indirect (inter-group, additive) singular vectors

$$\mathbf{H} = \overbrace{\mathbf{H}_D + \sum_g \mathbf{U}_{B,g} \boldsymbol{\Sigma}_{B,g} \underbrace{\mathbf{V}_{B,g}^H \boldsymbol{\Theta}_g \mathbf{U}_{F,g}}_{\text{backward-forward}} \boldsymbol{\Sigma}_{F,g} \mathbf{V}_{F,g}^H}^{\text{direct-indirect}}$$

Some concepts in differential geometry

The feasible domain of Θ_g is a unitary Lie group $U(L)$ with Lie algebra $\mathfrak{u}(L)$.

- *Geodesic*: shortest path between two points on a manifold
- *Lie group*: a group that is also a differentiable manifold
- *Lie algebra*: tangent space of Lie group at the identity element



A geodesic emanating from the identity with velocity $\mathbf{D} \in \mathfrak{u}(L)$ can be described by the exponential map

$$\mathbf{G}_I(\mu) = \exp(\mu\mathbf{D})$$

Geodesic RCG via Lie algebra

Non-geodesic vs geodesic Riemannian Conjugate Gradient (RCG)

- Non-geodesic: add then retract

$$\bar{\Theta}_g^{(r+1)} = \Theta_g^{(r)} + \mu \mathbf{D}_g^{(r)}, \quad \Theta_g^{(r+1)} = \bar{\Theta}_g^{(r+1)} (\bar{\Theta}_g^{(r+1)\text{H}} \bar{\Theta}_g^{(r+1)})^{-1/2}$$

- Geodesic: multiplicative and rotational update

$$\Theta_g^{(r+1)} = \mathbf{G}_g^{(r)}(\mu) = \exp(\mu \mathbf{D}_g^{(r)}) \Theta_g^{(r)}$$

Performance comparison

RCG path	$N_S = 16$			$N_S = 256$		
	Objective	Iterations	Time [s]	Objective	Iterations	Time [s]
Geodesic	4.359×10^{-3}	11.59	1.839×10^{-2}	1.163×10^{-2}	25.58	3.461
Non-geodesic	4.329×10^{-3}	30.92	5.743×10^{-2}	1.116×10^{-2}	61.40	13.50

Singular value redistribution: Optimization approach

Pareto frontier of singular values

$$\begin{aligned} \max_{\Theta} \quad & \sum_n \rho_n \sigma_n(\mathbf{H}) \\ \text{s.t.} \quad & \Theta_g^H \Theta_g = \mathbf{I}, \quad \forall g, \end{aligned}$$

Solution by group-wise geodesic RCG

- Faster convergence thanks to appropriate parameter space
- Step size μ can be obtained by the Armijo rule
- Doubling μ is computationally efficient $\exp(2\mu \mathbf{D}_g^{(r)}) = \exp^2(\mu \mathbf{D}_g^{(r)})$

Singular value redistribution: Analysis approach

Proposition (Degree of freedom)

In point-to-point MIMO, BD-RIS cannot achieve a higher Degree of Freedom (DoF) than diagonal RIS.

Proposition (Rank-deficient channel)

If the forward or backward channel is rank- k ($k \leq N$), then regardless of the passive RIS size and architecture, the n -th singular value of the equivalent channel is bounded by

$$\begin{aligned}\sigma_n(\mathbf{H}) &\leq \sigma_{n-k}(\mathbf{T}), & \text{if } n > k, \\ \sigma_n(\mathbf{H}) &\geq \sigma_n(\mathbf{T}), & \text{if } n < N - k + 1,\end{aligned}$$

where

$$\mathbf{T}\mathbf{T}^H = \begin{cases} \mathbf{H}_D(\mathbf{I} - \mathbf{V}_F\mathbf{V}_F^H)\mathbf{H}_D^H, & \text{if } \text{rank}(\mathbf{H}_F) = k, \\ \mathbf{H}_D^H(\mathbf{I} - \mathbf{U}_B\mathbf{U}_B^H)\mathbf{H}_D, & \text{if } \text{rank}(\mathbf{H}_B) = k, \end{cases}$$

and \mathbf{V}_F and \mathbf{U}_B are the right and left compact singular matrices of \mathbf{H}_F and \mathbf{H}_B , respectively.

Proposition (Unitary RIS without direct link)

If the BD-RIS is unitary and the direct link is absent, then the channel singular values can be manipulated up to

$$\text{sv}(\mathbf{H}) = \text{sv}(\mathbf{BF}),$$

where \mathbf{B} and \mathbf{F} are arbitrary matrices with the same singular values as \mathbf{H}_B and \mathbf{H}_F , respectively,

Achievable rate maximization

Problem formulation

$$\begin{aligned} \max_{\mathbf{W}, \Theta} \quad & R = \log \det \left(\mathbf{I} + \frac{\mathbf{W}^H \mathbf{H}^H \mathbf{H} \mathbf{W}}{\eta} \right) \\ \text{s.t.} \quad & \|\mathbf{W}\|_F^2 \leq P, \\ & \Theta_g^H \Theta_g = \mathbf{I}, \quad \forall g. \end{aligned}$$

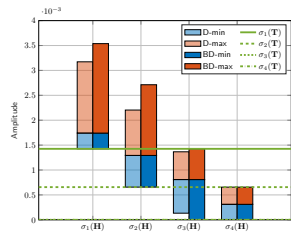
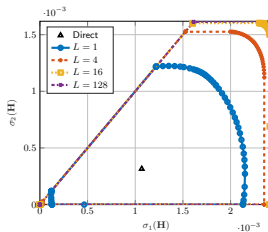
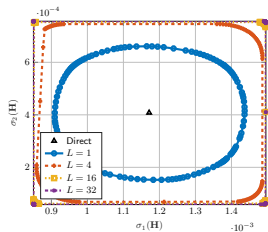
Local-optimal solution: BCD

- Passive beamforming Θ : group-wise geodesic RCG
- Active beamforming \mathbf{W} : eigenmode transmission and water-filling

Low-complexity solution: two-stage

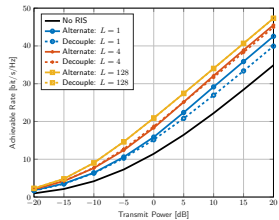
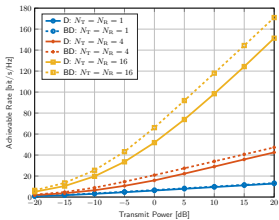
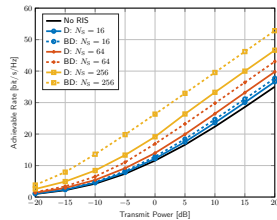
- Shaping stage: channel power gain maximization, solved in closed form
- Transmission stage: eigenmode transmission and water-filling

Simulation results: Singular value



- BD-RIS provides 22% and 38% dynamic range gain for $\sigma_1(\mathbf{H})$ and $\sigma_2(\mathbf{H})$
- Increasing group size enlarges singular value region with better trade-off
- Asymptotic bounds in rank-deficient channels are valid for both architectures

Simulation results: Achievable rate

(a) $4 \times 128 \times 4$ (b) $N_T \times 128 \times N_R$ (c) $4 \times N_S \times 4$

- Deficit from low-complexity design vanishes as RIS evolves towards unitary
- BD-RIS can activate multiple streams at lower transmit power
- Percentage rate gain of BD-RIS scales with MIMO dimension and group size

Future works: I

Coherent RISscatter detector

$$y[n] = \mathbf{h}_D^H + \mathbf{h}_C^H x \mathbf{w} s[n] + v[n],$$

- Same model as index modulation
- x has finite support $\rightarrow y[n]$ is a Gaussian mixture (non-elementary entropy)
- Achievable rate can be approximated as

$$R_B = \sum_i p(x_i) \log \sum_j p(x_j) \frac{4\sigma_i^2 \sigma_j^2}{(\sigma_i^2 + \sigma_j^2)^2}$$

- Bit Error Rate (BER) performance?
- Code-domain Non-Orthogonal Multiple Access (NOMA)?

Future works: II

Multiplicative broadcast channel

The received signal is

$$y_k = h_k \prod_q x_q + n.$$

- SIC → successive channel refinement (better symbol-level precoding)
- Log-normal is also maximum entropy distribution
- Product of log-normal is log-normal

Index modulation is a special case with superuser $R = R_1 + R_2$

- $x_1 \sim \mathcal{CN}(0, \sigma_1^2)$ and x_2 with finite support
- Index message encoded in the Euclidean distance between $hx_2^{(i)}$
- Decode x_2 first, rate depends on entropy of Gaussian mixture

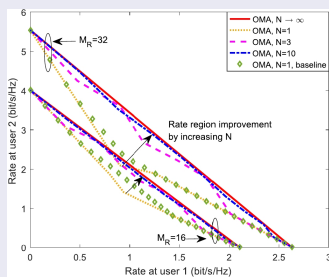
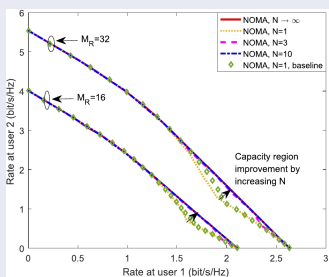
Future works: III

Rate splitting × index modulation

The received signal is

$$y_k = h_k \theta \sum_q x_q + n.$$

- Dynamic RIS achieves the convex hull below by time-sharing [7]



- Common message can be embedded in θ to push the boundary

Future works: IV

Feasibility of interference alignment by RIS

$$\begin{aligned} \text{find } \quad & \Theta \\ \text{s.t. } \quad & \mathbf{H}^{[kj]} = \mathbf{H}_{\text{D}}^{[kj]} + \mathbf{H}_{\text{B}}^{[k]} \Theta \mathbf{H}_{\text{F}}^{[j]} = \mathbf{0}, \quad \forall j \neq k \\ & \text{rank}(\mathbf{H}^{[kk]}) = d_k, \quad \forall k \end{aligned}$$

- Necessary and sufficient feasibility conditions?
- How many scattering elements are required on expectation?
- Multi-sector BD-RIS [8]?

-  Q. Wu and R. Zhang, "Towards smart and reconfigurable environment: Intelligent reflecting surface aided wireless network," *IEEE Communications Magazine*, vol. 58, pp. 106–112, Jan 2020.
-  R. Deng, F. Yang, S. Xu, and M. Li, "A low-cost metal-only reflectarray using modified slot-type phoenix element with 360° phase coverage," *IEEE Transactions on Antennas and Propagation*, vol. 64, pp. 1556–1560, Apr 2016.
-  S. Hu, C. Liu, Z. Wei, Y. Cai, D. W. K. Ng, and J. Yuan, "Beamforming design for intelligent reflecting surface-enhanced symbiotic radio systems," in *ICC 2022 - IEEE International Conference on Communications*, May 2022, pp. 2651–2657.
-  E. Arslan, I. Yildirim, F. Kilinc, and E. Basar, "Over-the-air equalization with reconfigurable intelligent surfaces," *IET Communications*, vol. 16, pp. 1486–1497, Aug 2022.
-  M. Trotter, J. Griffin, and G. Durgin, "Power-optimized waveforms for improving the range and reliability of RFID systems," in *2009 IEEE International Conference on RFID*, Apr 2009, pp. 80–87.
-  B. Molina-Farrugia, A. Rivadeneyra, J. Fernández-Salmerón, F. Martínez-Martí, J. Banqueri, and M. A. Carvajal, "Read range

enhancement of a sensing RFID tag by photovoltaic panel," *Journal of Sensors*, vol. 2017, pp. 1–7, 2017.

-  X. Mu, Y. Liu, L. Guo, J. Lin, and N. Al-Dhahir, "Capacity and optimal resource allocation for IRS-assisted multi-user communication systems," *IEEE Transactions on Communications*, vol. 69, pp. 3771–3786, Jun 2021.
-  H. Li, S. Shen, and B. Clerckx, "Beyond diagonal reconfigurable intelligent surfaces: A multi-sector mode enabling highly directional full-space wireless coverage," *IEEE Journal on Selected Areas in Communications*, vol. 41, pp. 2446–2460, Aug 2023.